EWRA

EUROPEAN WATER RESOURCES ASSOCIATION

10th WORLD CONGRESS

on Water Resources and Environment

"Panta Rhei"

5-9 July 2017
Athens, Greece

PROCEEDINGS

Editors

George Tsakiris
Vassilios A. Tsihrintzis
Harris Vangelis
Dimitris Tigkas

Athens, 2017

EUROPEAN WATER RESOURCES ASSOCIATION

10th WORLD CONGRESS
on Water Resources and Environment

"Panta Rhei"

5-9 July 2017
Athens, Greece

PROCEEDINGS

Editors

George Tsakiris
Vassilios A. Tsihrintzis
Harris Vangelis
Dimitris Tigkas

Athens, 2017

A.R.Kacimov, A.Al-Maktoumi, Yu.V.Obnosov. Phreatic/Confined Flows in Polygons: Dupuit-Forchheimer Model Versus Potential Solutions.
Proceedings of the 10th World Congress of EWRA 'Panta Rhei'; 5-9 July 2017, Athens, Greece, pp.1987-1994.

Proceedings of the 10th World Congress of EWRA 'Panta Rhei', 5-9 July 2017, Athens, Greece

Phreatic / confined flows in polygons: Dupuit-Forchheimer model versus potential solutions

A.R. Kacimov[1*], A. Al-Maktoumi[1] and Y.V. Obnosov[2]
[1] Department of Soils, Water and Agricultural Engineering, Sultan Qaboos University, Oman
[2] Institute of Mathematics and Mechanics, Kazan Federal University, Kazan, Russia
[*] e-mail: anvar@squ.edu.om

Abstract: Analytical and numerical (HYDRUS2D and MODFLOW) solutions for steady unconfined Darcian flows with accretion and leakage in a single aquifer is obtained for domains bounded by trigons (in particular common triangles) and polygons that allows modeling catchment-scale groundwater flows. Strack's comprehensive potential obeys the 2-D Poisson equations, which assumes the Dupuit-Forchheimer vertical averaging of the head. Along the lateral boundaries in 2-D flows and leaky layer in 1-D flow, Robin's condition models clogging of river/wadi banks and beds. In a layered aquifer, confined flows are decoupled into two types of analytic elements: highly-low permeable strata with 1-D and essentially 2-D seepage, correspondingly. The conjugation between these fragments is based on a "seepage shear" condition. This leads to a boundary condition along the interfaces between the two types of commingled strata, which is similar to Kirkham-Brock's one. The method of hodograph is used for two types of 2-D potential flow fragments: arbitrary triangles and trapezia. By routines of computer algebra, the complex potential and physical domain are parametrized via an auxiliary variable. Deviation from trivial 1-D approximations in 2-D fragments are found. Implications for groundwater quality, dissolution of the porous skeleton of the strata and soil erosion by suffusion, as triggered by an intricate "winding" of flow paths between the strata, are discussed.

Key words: Seepage refraction, hodograph, leaky layer, infiltration, numerical simulations

1. INTRODUCTION

In groundwater hydrology and geotechnical/reservoir engineering, steady Darcian flows through saturated porous materials often involve a basic analytic element of a stratified domain consisting of two rectangular horizontal layers OB_1B_2C and OCC_1O_1 of contrasting hydraulic conductivities, K_1 and K_2, sandwiched between an impermeable bedrock and caprock (Fig.1).

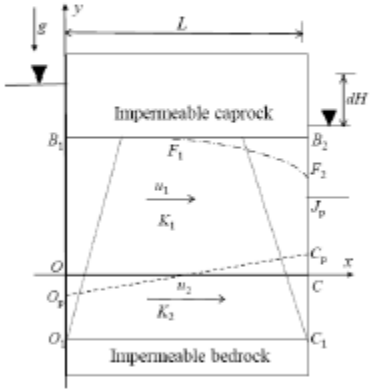

Figure 1. Two-layered aquifer.

If the inlet O_1OB_1 and outlet C_1CB_2 are vertical and "fully submerged" under the corresponding left-right river levels, then flow in both strata of Fig.1 is strictly horizontal and not commingled. The Darcian velocities $u_1=K_1\,dH/L$ and $u_2=K_2\,dH/L$ do not depend on each other and there is no cross-flow from one layer to another. Then the stream tubes are rectangles, with the stremalines parallel to the interface.

In aquifers, soils, earth dams and even laminated porous chemical reactors the ideal conceptualization of Fig.1 does not realize and gravity, multiple external inputs (leakage through aquitards, infiltration-evaporation, unsaturated zones, among others) distort the 1-D flow regimes and then gravity, Darcian resistance and capillarity make complicated topology of water fluxes and fields of state variables (pore pressure, velocity, moisture content, temperature, concentration of dissolved solutes) as investigated in Polubarinova-Kochina (1977), Strack (1989) and Toth (2009).

In this paper, we study one-phase water/moisture flows in rigid aquifers and the following physical perturbations of the trivial 1-D flows in Fig. 1:

a) The interface OC can be tilted (a dashed line O_pC_p in Fig.1);
b) The inlet and outlets (dotted lines O_1B_{1p} and C_1B_{2p}) can be non-vertical;
c) The water level in the rivers of Fig.1 can drop beneath the bedrock (for example, point B_2 drops to point J_p) such that a phreatic surface F_1F_2 (dashed-dotted line) and seepage face F_2J_p are formed;
d) The confining upper and lower rocks can be slightly permeable and accretion or losses from layers 1 and 2 can take place as infiltration or leakage;
e) The segments O_1B_1 and C_1B_2 can be "clogged" by a thin layer of low-permeable sediments.

The impact of perturbation a) has been addressed in Kacimov and Obnosov (1995, 1997, 2000, 2012), Kacimov et al. (1999) as the problem of refraction (conjugation) of two 2-D confined flows. In refraction, the normal component of the Darcian velocity vectors and pore pressures across O_pC_p are continuous but the velocity components tangential to the interface jump. Only in view types of tilted interfaces O_pC_p exact analytical solutions are possible. Therefore, simplified analytical analysis of perturbations b)-e) calls for benchmarking with numerical solutions. Our main assumption is: the substratum of conductivity K_2 or clogging of the riverbank is thin and flow there is 1-D and either along or across the layer.

2. TWO-DIMENSIONAL FLOW IN TRIANGULAR SEEPAGE-FACED DOMAIN WITH THIN "SHEARING" SUBSTRATUM

In this section we consider a special case of a two-layered conduit in Fig. 1: a relatively low permeable triangle OBC and a highly-permeable subjacent trapezium O_1OCC_1 (Fig.2a). The segment BC_1 is a seepage face. We introduce Cartesian coordinates xOy, the abscissa axis coinciding with the interface. The trapezium (Fig.2b) has a small thickness d and the upper base OC of a size $L=H(\cot\pi\alpha+\cot\pi\gamma)$. The middle line of the trapezium is L_1, $L_1>L$. We assume that flow in the trapezium is 1-D, horizontal (along the layer) and not affected by flow in the triangle. This assumption holds if $K_2>>K_1$. In the superjacent triangle, flow is 2-D and is influenced by the "seepage shear" in the trapezium (see Kacimov, 2006).

We approximate the sides O_1O and C_1C of the trapezium in Fig. 2b as vertical segments (in reality they are not) and C_1C as a constant head outlet (although this line is a seepage face). Then from Darcy's law the velocity in the trapezium can be approximated as:

$$u_2 = K_2H_0 / L_1 \tag{1}$$

The triangle OBC, G_z, has angles $\alpha\pi$, $\beta\pi$ and $\gamma\pi$ (clearly, $\alpha+\beta+\gamma=1$), and height $H=H_0-d$. We consider the case $\beta<\pi/2$. Davison (see Khristianovich et al., 1938) studied flow in triangular cores assuming that OC in Fig.2a is a no-flow boundary. In this paper, the boundary condition along OC

is determined from the refraction condition of two commingled flows: a 2-D in G_z and approximate 1-D in the subjacent trapezium. The horizontal component u_1 of the velocity vector $V_1(u_1,v_1)$ in G_z obeys the following conjugation boundary condition along OC (Polubarinova-Kochina, 1977):

$$u_1 / K_1 = u_2 / K_2 \tag{2}$$

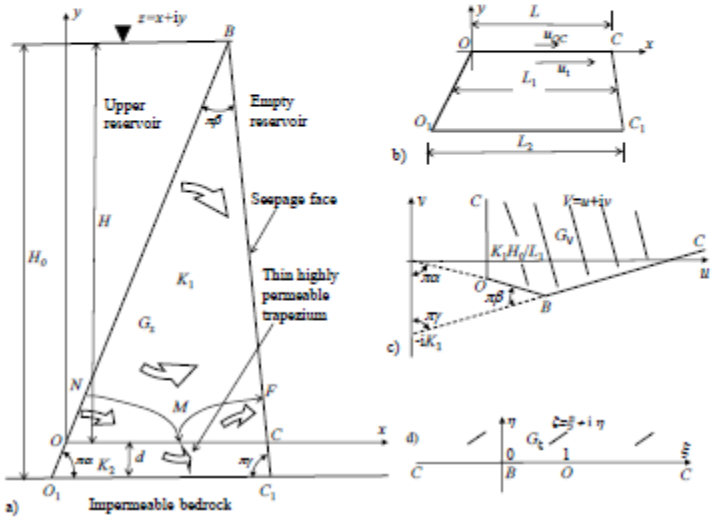

Figure 2. Vertical cross-section of flow through two commingles porous fragments (a), trapezoidal substratum (b), hodograph domain for 2-D flow in triangle, auxiliary complex plane (d).

From Eqs. (1) and (2) the horizontal component of velocity along the bottom of the triangle is:

$$u_{OC} = K_1 H_0 / L_1 \tag{3}$$

This condition is analogous to the Kirkham-Brock boundary condition of a constant vertical component of velocity at the bottom of a porous flow domain with a very low-permeable underlay (Kacimov and Obnosov, 2015).

For flow in the triangle G_z, we introduce a complex physical plane $z=x+iy$ and complex potential $w=\phi+i\psi$ ($\phi=-K_1 h$, $h=p+y$, h is the total hydraulic head and p is the pressure head). A complexified Darcian velocity is $V=u+iv$ (we drop the subscript "1"). The hodograph domain G_V in Fig. 2c is a trigon whose angles are determined as in Polubarinova-Kochina (1977). According to Eq. (3), the vertical ray OMC passes through the point V_M=const=K_1H_0/L. The domain G_ω, ω=dw/dz, is a mirror image of G_V with respect to the horizontal axis. We map conformally G_ζ the upper half of an auxiliary ζ-plane, onto G_z (see Fig.2d) by the Schwartz-Christoffel transformation:

$$z(\zeta) = -c_1 e^{i\pi\alpha} \int_1^{\zeta} \tau^{\beta-1}(1-\tau)^{\alpha-1} d\tau = c_1 e^{i\pi\alpha} \int_0^{1-\zeta} \tau^{\alpha-1}(1-\tau)^{\beta-1} d\tau \tag{4}$$

The positive mapping constant c_1 in eqn. (4) is determined by the condition $z(0)=H$ ($\cot\pi\alpha+i$) as:

$$c_1 = \frac{H}{\sin\pi\alpha} \Big/ \int_0^1 \tau^{\beta-1}(1-\tau)^{\alpha-1}\,\mathrm{d}\tau = \frac{H}{\sin\pi\alpha\, B(\alpha,\beta)}$$

Then Eq. (4) upon integration becomes:

$$z(\zeta) = e^{i\omega}\frac{H\,\mathrm{B}(1-\zeta;\alpha,\beta)}{\sin\pi\alpha\,\mathrm{B}(\alpha,\beta)} \tag{5}$$

Here $\mathrm{B}(\alpha,\beta)$ is the Euler beta function and $\mathrm{B}(z;\alpha,\beta)$ is the incomplete beta function. At point C the width $L = z(\infty) = H(\cot\pi\alpha + \cot\pi\gamma)$.

The boundary conditions for an analytic function ω=dw/dz=u- iv are:

BC: v=cot$\pi\gamma$ u - K_1
OB: $v = -\cot\pi\alpha\ u$
OC: u=K_1H_0 / L_1

wherefrom we get:

$$V_B = u_B + \mathrm{i}v_B = \frac{K_1}{\cot\pi\alpha + \cot\pi\gamma} - \mathrm{i}\frac{K_1\cot\pi\alpha}{\cot\pi\alpha + \cot\pi\gamma} = -\mathrm{i}e^{i\omega}K_1\frac{\sin\pi\gamma}{\sin\pi\beta},$$
$$V_O = u_O + \mathrm{i}v_O = \frac{K_1H_0}{L_1} - \mathrm{i}\frac{K_1H_0}{L_1}\cot\pi\alpha = -\mathrm{i}e^{i\omega}\frac{K_1H_0}{L_1\sin\pi\alpha}.$$

Similarly, taking into account that $B = \mathrm{i}e^{-i\omega}K_1\sin\pi\gamma / \sin\pi\beta$, we map G_ζ onto G_* by the Schwartz-Christoffel integral:

$$\omega(\zeta) = \mathrm{d}w/\mathrm{d}z = -\mathrm{i}e^{-i\omega}\left(c_2\int_0^\zeta \tau^{-\beta}(1-\tau)^{-\alpha}\,\mathrm{d}\tau - \frac{K_1\sin\pi\gamma}{\sin\pi\beta}\right) \tag{6}$$

where the positive mapping constant c_2 has to be found from the given position of point $O = \omega(1) = \mathrm{i}e^{-i\omega}K_1H_0 / (L_1\sin\pi\alpha)$ in G_*. Then Eq. (6) upon integration transforms to:

$$\mathrm{d}w/\mathrm{d}z = -\mathrm{i}e^{-i\omega}\frac{K_1\sin\pi\gamma}{\sin\pi\beta}\left(\frac{H_0}{H}\frac{\mathrm{B}(\zeta;1-\beta,1-\alpha)}{\mathrm{B}(1-\beta,1-\alpha)}\left(1-L/L_1\right)-1\right) \tag{7}$$

From Eqs. (5) and (7) we get:

$$w(\zeta) = \int_1^\zeta \frac{\mathrm{d}w}{\mathrm{d}z}\frac{\mathrm{d}z}{\mathrm{d}\zeta}\mathrm{d}\zeta = -\frac{e^{i\omega}H}{\sin\pi\alpha\,\mathrm{B}(\alpha,\beta)}\int_1^\zeta \frac{\mathrm{d}w}{\mathrm{d}z}\zeta^{\beta-1}(1-\zeta)^{\alpha-1}\mathrm{d}\zeta$$

$$w(\zeta) = \mathrm{i}\frac{\gamma K_1}{\pi}\left[\left(1-L/L_1\right)H_0\int_1^\zeta \frac{\mathrm{B}(t;1-\beta,1-\alpha)}{t^{1-\beta}(1-t)^{1-\alpha}}\mathrm{d}t - H\,\mathrm{B}(1-\beta,1-\alpha)\,\mathrm{B}(1-\zeta;\beta,\alpha)\right] \tag{8}$$

where w_O=w(1)=0. Therefore, the flow rate through OB is:

$$\psi_B = \mathrm{Im}\, w(0) = K_1\left[H\frac{\sin\pi(\alpha+\beta)}{\sin\pi\alpha\sin\pi\beta} - \frac{\gamma}{\pi}\left(1-L/L_1\right)H_0\int_0^1 \frac{\mathrm{B}(t;1-\beta,1-\alpha)}{t^{1-\beta}(1-t)^{1-\alpha}}dt\right] \tag{9}$$

i.e. ψ_B depends linearly on L/L_1.

We used Eq. (7) for plotting the magnitude of the Darcian velocity vector along *OC* in Fig.2. If this vector is oriented from the triangle into the substratum and the hydraulic gradient exceeds a safe limit (Polubarinova-Kochina, 1977 suggested this limit to be 1) an internal erosion across the interface takes place. This insidious phenomenon (suffusion) is much more difficult to combat than a common "visible" erosion along BC_1 (see Yakimov and Kacimov, 2017). In Fig. 2, a separatrix *NMF* divides flow into a part which passes through the first medium only and a "winding" part which dives into and re-emerges from the substratum. This topology is of concern in evaluations of groundwater quality which depends on the residence time of water particles within a specific hydrostratigraphic unit.

3. ONE-DIMENSIONAL DUPUIT-FORCHHEIMER FLOW IN LEAKY AQUIFER WITH ACCRETION

In this section we consider perturbation c). Without any loss of generality, we assume the water levels in both rivers of Fig.1 below the caprock and being constant, h_L (Fig.3). The caprock is slightly permeable and infiltrates with a given intensity of $N>0$ that recharges the phreatic surface *BC*. The horizon H=const>0 in Fig.3 is determined by a constant total hydraulic head H in the deeper aquifer which supplies water through a leaky layer. Due to symmetry the watershed between the two rivers is considered as the *Oy* axis.

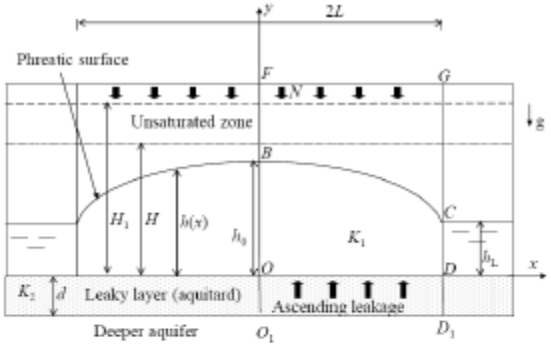

Figure 3. Vertical cross-section of phreatic flow with leaky layer and infiltration.

Recently, Strack (2017) and Ausk and Strack (2015) investigated stratified aquifers similar to one in Fig.3 using the Dupuit-Forcheimer model. In this model, flow is vertically averaged that results in the following boundary-value problem for an ordinary differential equation (ODE):

$$K_1\frac{\mathrm{d}}{\mathrm{d}x}\left(h\frac{\mathrm{d}h}{\mathrm{d}x}\right) = \frac{K_2}{d}(h-H) - N, \quad 0 \le x \le L,$$
$$h(L) = h_L, \qquad \frac{\mathrm{d}h}{\mathrm{d}x}(0) = 0, \tag{10}$$

where $h(x)$ is the saturated thickness measured from *OD* in Fig.3. Leakage from a deeper aquifer is counted through the Robin boundary condition (the first term in the RHS of eqn.(10)). We introduce

$\omega = \sqrt{K_2 / (K_1 dH_1)}$, H_1=H+Nd/K_2, the maximum water table height is h_0. Dimensionless variables are: $(h^*, h_0^*, h_L^*, x^*, L^*) = (h/H_1, h_0/H_1, h_L/H_1, \omega x, \omega L)$. We drop the superscript "*" for the sake of brevity. Then Eq. (10) becomes a nonlinear ODE:

$$\frac{\mathrm{d}}{\mathrm{d}x}\left(h\frac{\mathrm{d}h}{\mathrm{d}x}\right) = h - 1. \tag{11}$$

We followed Rybakova and Emikh (1966) and linearised Eq. (10) by multiplying it by $(h+1)/(2h_a)$ where $h_a = (h_0 + 1)/2$. The resulting linear ODE is integrated as:

$$h^2 = 1 - (1 - h_L^2)\frac{\cosh(x/\sqrt{h_a})}{\cosh(L/\sqrt{h_a})}. \tag{12}$$

At x=0 Eq. (12) reads:

$$h_0^2 = 1 - (1 - h_L^2)\frac{1}{\cosh[L/\sqrt{(h_0+1)/2}]} \tag{13}$$

which is a nonlinear equation with respect to h_0. We solved Eq. (13) by computer algebra and compared the results with the solution of the non-linear Eq. (11), which dates back to Boussinesq (see Polubarinova-Kochina, 1977). We showed that the water tables in the two cases practically coincide.

We also used HYDRUS2D FEM code (Šimůnek et al., 2008) and simulated a transient saturated-unsaturated flow governed by the Richards equation. We selected a rectangular domain O_1FGDD_1 (Fig. 3) of sizes $2L$=20 m and $|OF|$=2 m. This rectangle is composed of a thin silty clay layer O_1ODD_1 of conductivity K_2=0.48 cm/day, d= 20 cm, and an overlying coarser layer $OFGD$, a sandy loam with K_1 = 106 cm/day, 180 cm thick. The initial condition in terms of the pressure head is p_0=-100 cm. The flow domain discretization was 20 and 10 layers in x- and z- directions. The boundary conditions for the right half of the flow domain in Fig. 3 are: a constant total head h_L=60 cm along CD, no flux along O_1OF and D_1D, vertical infiltration flux N=2 cm/day along FG, seepage face condition along CG, and constant positive pressure head p=80 cm along O_1D_1. The Van Genuchten-Mualem soil properties are selected for both strata from the Soil Catalogue of HYDRUS.

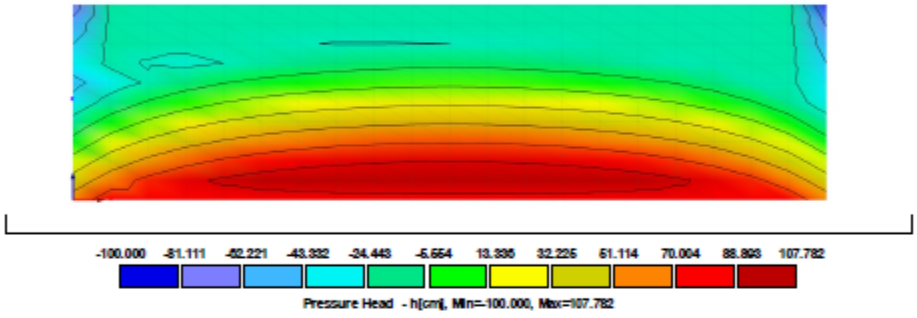

Figure 4. HYDRUS2D calculated pore pressure head in a vertical cross-section of Fig. 3.

HYDRUS2D gives distributions of $p(x,y,t)$ (Fig. 4), moisture content, $m(x,y,t)$, velocity magnitude, $V(x,y,t)$ and its horizontal $u(x,y,t)$ and vertical $v(x,y,t)$ components. Simulations were run for 40 days and steady-state flow established in about 20 days that was monitored at a set of observational nodes within the rectangles. HYDRUS2D-computed steady-state h_0 is almost the same as in the analytical solution, Eq. (12). The Dupuit-Forchheimer model does not, obviously, predict the vertical variation of the total head $h(x,y)$ or $V(x,y)$, as HYDRUS2D or the potential model in Section 2 do. From Fig.4 we see that at steady state conditions there is a distinct maximum of the pore pressure $p(0,y)$= 108 cm just above point O in Fig. 3. Similarly to Section 2, we checked that the hydraulic gradient at the interface between the fine substratum and coarser layer is within the suffusion limit.

4. TWO-DIMENSIONAL DUPUIT-FORCHHEIMER FLOW IN A TRIANGULAR AQUIFER WITH ACCRETION AND CLOGGED RIVER BANKS.

In Section 3 the groundwater mound was symmetric with respect to the discharge outlets (parallel rivers) and in the "leaky" substratum (aquitard) of Fig.4 flow was 1-D vertical posited in eqn. (10). The discharge boundary may have a polygonal shape that corresponds to islands, promontories, meandering rivers, among others. In this Section, we model 2-D Dupuit-Forchheimer flow with accretion on the phreatic surface in the same triangular domains as in Kacimov et al. (2016), with the following difference: along the river banks (the triangle boundary) the Robin rather than Dirichlet's boundary condition holds. In other words, flow through clogged river banks is normal to the triangle sides and the flux is proportional to the head difference in the aquifer (unknown and varying along the triangle sides) and river (fixed and known).

A numerical solution has been obtained by a MODFLOW-based FDM (Simcore Software, 2012). A regular triangular domain was considered. All external boundaries of the triangle are constant head river boundaries. The hydraulic head in the river (triangle's exterior) is 9 m whereas the initial head in the aquifer (triangle's interior) is 10 m, the triangle height is 300 m, K_1 =10 m/day for the aquifer and K_2= 1 m/day for the clogging layer of the river bank, the recharge rate N=0.09 m/day, aquifer's porosity =0.35, and the aquifer thickness is 20 m. The grid cells are uniform in the x- and y- directions: $dx = dy$ = 3 m away from the triangle sides. The grid is refined to $dx = dy$ = 1m as the triangle boundary is approached. This results in a mesh of 134 rows and 150 columns, the total number of active cells is 46503 with a volume of 930060 m^3. The Preconditioned Conjugate Gradient (*PCG2*) solver has been selected for solving the flow equation with a convergence criterion of 0.001.

The MODFLOW calculated water table surface is shown in Fig. 5a and the head distribution line at a cross section A-A` is presented by Fig. 5b.

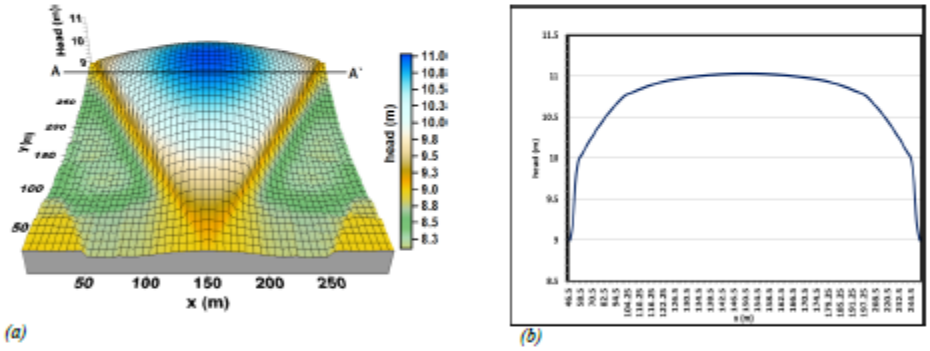

(a) (b)

Figure 5. (a) MODFLOW calculated 3-D water table surface; (b) water table across the cross-section A-A`.

MODFLOW simulation results illustrate that the clogged riverbank induces a water table mound with a maximum at the centre of the triangle significantly higher than that for the constant head bank (Kacimov et al., 2016). The low permeability "cake" of the river-bank causes a steep hydraulic gradient at the aquifer-riverbank interface ($dh/dx=0.175$), a lower than 0.02 gradient elsewhere in the domain (with a minimum reaching a value of 0.0001 across cells at the apex of the mound.

5. CONCLUDING REMARKS

Analytical and numerical solutions obtained for steady-state or asymptotic steady-state limits of transient saturated or saturated-unsaturated flows, if juxtaposed, provide insight of a complex topology and field values of groundwater characteristics: total head, pore pressure, and Darcian velocity in aquifers of polygonal geometry, both in a vertical and planar cross-sections. The corresponding simulations are indispensable tools in water resource management.

REFERENCES

Kacimov A.R. 2006. Analytical solution and shape optimisation for groundwater flow through a leaky porous trough subjacent to an aquifer. Proc. Royal Soc. London A, 462, 1409-1423.

Kacimov A.R., Obnosov Yu.V. 1995. Groundwater flow in a medium with periodic inclusions. Fluid Dynamics, 30(5), 758-766.

Kacimov A.R., Obnosov Yu.V. 1997. Analytic solution to a problem of seepage in a checker- board massif. Transport in Porous Media, 28 (1), 109-124.

Kacimov A.R., Obnosov Yu.V. 2000. Two-dimensional seepage in porous media with heterogeneities. J. Geochemical Exploration, 69-70, 251-255.

Kacimov A., Kayumov I., Al-Maktoumi A. 2016. Rainfall induced groundwater mound in wedge-shaped promontories: the Strack-Chernyshov model revisited. Advances in Water Resources, 2016, 97, 110-119.

Kacimov A.R., Obnosov Yu.V., Yakimov N.D. 1999. Groundwater flow in a medium with a parquet-type conductivity distribution. J. Hydrology, 226, 242-249.

Kacimov A.R., Obnosov Yu.V. 2012. Analytical solutions for seepage near material boundaries in dam cores: the Davison-Kalinin problems revisited. Applied Mathematical Modelling, 36, 1286–1301.

Kacimov A.R., Obnosov Yu.V. 2015. An exact analytical solution for steady seepage from a perched aquifer to a low-permeable sublayer: Kirkham-Brock's legacy revisited. Water Resources Research, 51, 3093–3107.

Khristianovich, S.A., Mikhlin S.G. and Davison B.B. 1938. Some New Problems of Continuum Mechanics. Moscow-Leningrad, Akad. Nauk SSSR (in Russian).

Polubarinova-Kochina, P.Ya. 1977. Theory of Ground-water Movement. Nauka, Moscow (in Russian).

Rybakova S.T., Emikh V.N. 1966. On the problem of horizontal perfect drainage with a leaky layer. Izv. An SSSR Mekhanika Zhidkosti i Gaza, N3, 161-165 (in Russian).

Simcore Software, 2012. Processing MODFLOW: an integrated modeling environment for the simulation of groundwater flow. Transport React. Process.

Šimůnek J., Van Genuchten M.T., Šejna, M. 2008. Development and applications of the HYDRUS and STANMOD software packages and related codes. Vadose Zone J., 7(2), 587–600.

Strack O. D. L. 1989. Groundwater Mechanics. Prentice-Hall, Englewood Cliffs.

Strack O.D. 2017. Vertically integrated flow in stratified aquifers. J. Hydrology (in press).

Strack O.D.L., Ausk B.K. 2015. A formulation for vertically integrated groundwater flow in a stratified coastal aquifer. Water Resources Research, 51(8), 6756-6775.

Toth, J. 2009. Gravitational Systems of Groundwater Flow- Theory, Evaluation, Utilization. Cambridge University Press, Cambridge.

Yakimov N.D., Kacimov A.R. 2017. Darcian flow under/through a leaky cutoff-wall: Terzaghi-Anderson's seepage problem revisited. International J. for Numerical and Analytical Methods in Geomechanics, DOI: 10.1002/nag.2668